

# The Interaction Properties of Costimulatory Molecules Revisited

Alison V. Collins,<sup>1,7</sup> Douglas W. Brodie,<sup>2,7</sup>  
Robert J.C. Gilbert,<sup>3,4</sup> Andrea Iaboni,<sup>1</sup>  
Raquel Manso-Sancho,<sup>1</sup> Björn Walse,<sup>5</sup>  
David I. Stuart,<sup>3,4</sup> P. Anton van der Merwe,<sup>2,6</sup>  
and Simon J. Davis<sup>1,6</sup>

<sup>1</sup>Nuffield Department of Clinical Medicine  
The University of Oxford  
John Radcliffe Hospital  
Headington  
Oxford OX3 9DU

<sup>2</sup>Sir William Dunn School of Pathology  
The University of Oxford  
South Parks Road  
Oxford OX1 3RE

<sup>3</sup>Division of Structural Biology  
The Henry Wellcome Building for Genomic Medicine  
The University of Oxford  
Roosevelt Drive  
Oxford OX3 7BN

<sup>4</sup>Oxford Centre for Molecular Sciences  
The University of Oxford  
New Chemistry Laboratory  
South Parks Road  
Oxford OX1 3QT  
United Kingdom

<sup>5</sup>Active Biotech Research AB  
Scheelevägen 22363, Lund  
Sweden

## Summary

**B7-1 and B7-2 are generally thought to have comparable structures and affinities for their receptors, CD28 and CTLA-4, each of which is assumed to be bivalent. We show instead (1) that B7-2 binds the two receptors more weakly than B7-1, (2) that, relative to its CTLA-4 binding affinity, B7-2 binds CD28 2- to 3-fold more effectively than B7-1, (3) that, unlike B7-1, B7-2 does not self-associate, and (4) that, in contrast to CTLA-4 homodimers, which are bivalent, CD28 homodimers are monovalent. Our results indicate that B7-1 markedly favors CTLA-4 over CD28 engagement, whereas B7-2 exhibits much less bias. We propose that the distinct structures and binding properties of B7-1 and B7-2 account for their overlapping but distinct effects on T cell responses.**

## Introduction

Immune responses are profoundly influenced by protein interactions involving leukocyte cell surface proteins. Prominent among these are the B7 ligands, B7-1 (CD80) and B7-2 (CD86) expressed on antigen-presenting cells,

and their receptors, CD28 and CTLA-4 (CD152) expressed by T cells (reviewed by Lenschow et al., 1996). An additional CD28-like molecule, ICOS (Hutloff et al., 1999), interacts with another B7-related molecule, LICOS (Brodie et al., 2000), known also as B7h, B7RP-1, and GL-50 (reviewed by Mueller, 2000). However, binding studies (Brodie et al., 2000) and the analysis of transgenic mice (Mandelbrot et al., 1999) indicate that B7-1 and B7-2 are the only functional ligands of CD28 and CTLA-4. CD28 is constitutively expressed on most resting human T cells, and B7-2 is rapidly induced on antigen-presenting cells early in immune responses. The expression of B7-1 and CTLA-4 generally occurs only after a delay of 24–48 hr, however (reviewed by Lenschow et al., 1996).

CD28 and CTLA-4 are expressed at the cell surface as covalent homodimers of single V-set immunoglobulin superfamily (IgSF) domains, whereas B7-1 and B7-2 each consist of single V-set and C1-set IgSF domains (reviewed by Lenschow et al., 1996; Ikemizu et al., 2000). It is clear that CTLA-4 binds bivalently to B7-1 and B7-2 (Schwartz et al., 2001; Stamper et al., 2001), but the stoichiometry of CD28 interactions is poorly defined. Crystallographic and solution studies indicate that soluble (s) B7-1 tends to dimerize, prompting the suggestion that, at the cell surface, the interactions of B7-1 might be avidity-enhanced by the formation of two-dimensional arrays in which B7-1 homodimers are bridged by bivalent ligand (Ikemizu et al., 2000). The affinity of sB7-1 self-association is consistent with B7-1 existing at the cell surface in a dynamic equilibrium dominated by the dimer (Ikemizu et al., 2000).

CD28 belongs to a group of molecules that “costimulate” T cells. In the absence of such signals, T cells enter an anergic state (reviewed by Jenkins, 1994). CD28 signaling synergizes with that of the T cell receptor (TCR) to induce cell proliferation and cytokine secretion. Specifically, CD28 and TCR signals intersect in a Vav1-dependent manner before inducing the binding of NF- $\kappa$ B/Rel- and AP-1-family transcription factors to a composite CD28 response element in the IL-2 promoter (Shapiro et al., 1997; Hehner et al., 2000). CD28 also stabilizes IL-2 mRNA and enhances T cell survival by increasing the expression of the antiapoptotic protein, Bcl-xL (Lindstein et al., 1989; Boise et al., 1995). Finally, the pro-signaling microenvironment of the immunological synapse is enhanced by the recruitment of cell surface molecules and kinase-rich rafts in response to costimulatory signaling (Wülfing and Davis, 1999; Viola et al., 1999). CTLA-4 engagement, on the other hand, induces powerful inhibitory signals in T cells as is best illustrated by the severe lymphoproliferative disorder to which CTLA-4-deficient mice succumb shortly after birth (Waterhouse et al., 1995). CTLA-4 attenuates I $\kappa$ k, fyn, and ZAP-70 activation and has been linked to dephosphorylation of the  $\zeta$  chain of CD3 (Marengere et al., 1996; Lee et al., 1998). Other data suggest that CTLA-4 inhibits T cell activation, at least in part, by competing with CD28 for ligands on antigen-presenting cells (Masteller et al., 2000). In addition to these proximal effects

<sup>6</sup>Correspondence: anton.vandermerwe@path.ox.ac.uk (P.A.v.d.M.), sdavis@molbiol.ox.ac.uk (S.J.D.)

<sup>7</sup>These authors contributed equally to this work.

on signaling, CTLA-4 may mediate its inhibitory effects indirectly, possibly by enhancing the generation of regulatory CD25<sup>+</sup> T cells (Bachmann et al., 1999; Read et al., 2000; Takahashi et al., 2000).

Although the activating and inhibitory functions of CD28 and CTLA-4 ligation are well established, the requirement for the two sequentially expressed ligands, B7-1 and B7-2, is poorly understood. It is clear that the genes encoding B7-1 and B7-2 arose via duplication of a common precursor and that the functions of B7-1 and B7-2 overlap considerably (see, e.g., Borriello et al., 1997). The preservation of both genes in all mammals examined, however, strongly suggests that the two genes have been subjected to distinct selection pressures. Moreover, numerous studies have documented the differential effects of anti-B7-1 and anti-B7-2 blocking antibodies on immune responses both in vitro and in animal models (reviewed by Lenschow et al., 1996; Salomon and Bluestone, 2001). Nevertheless, there is little consensus regarding whether or not B7-1 and B7-2 have distinct regulatory functions and even less agreement on what these functions might be.

At least part of the explanation for this is that there has been no obvious molecular basis for large functional differences, given that the interactions of costimulatory molecules are generally thought to have relatively uniform properties, i.e., that B7-1 and B7-2 have similar structures and affinities for CD28 versus CTLA-4 and that CD28 and CTLA-4 are both bivalent (see Sharpe and Freeman, 2002 and Carreno and Collins, 2002, for the prevailing view). We show here that costimulatory receptors and their ligands in fact form signaling complexes of unexpected structural diversity, whose stabilities vary by more than four orders of magnitude. Our results are consistent with a model of T cell costimulation in which the distinct structures and binding properties of B7-2 and B7-1 significantly enhance the activating and inhibitory functions of CD28 and CTLA-4, respectively.

## Results

### Expression of sB7-2

Soluble, histidine-tagged B7-2 (sB7-2) was expressed in Chinese hamster ovary (CHO) cells using the approach followed for sB7-1 (van der Merwe et al., 1997). Truncation of the protein at Pro-224 yielded a product consisting of the intact extracellular region of B7-2. In reducing and nonreducing SDS-PAGE gels, sB7-2 migrated as a broad band of 45–60 kDa (Figure 1A), consistent with heavy glycosylation (at up to eight sites). The sB7-2 was completely depleted from solution by conformation-sensitive, noncompeting anti-B7-2 monoclonal antibodies (mAbs: BU63 and FUN-1; Figure 1B) and crystallized (data not shown), implying that all of the purified protein was correctly folded. CD28 and CTLA-4, expressed as chimeras with human IgG Fc (designated CD28Fc and CTLA-4Fc, respectively), are characterized elsewhere (van der Merwe et al., 1997). A second CD28Fc chimera, consisting of the entire extracellular region of CD28 (inclusive of the native, interchain disulfide), a thrombin-cleavable site, and murine IgG Fc, will be described elsewhere (R.M.-S. et al., unpublished data).

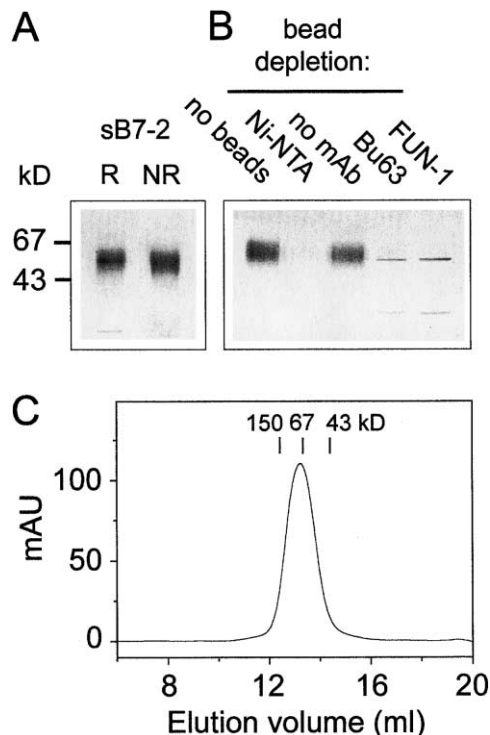


Figure 1. Characterization of sB7-2

(A) SDS-PAGE analysis of sB7-2 under reducing (R) and nonreducing (NR) conditions. Distances that reduced molecular weight markers migrated are indicated.

(B) Depletion of a solution of purified sB7-2 (lane 1) by Ni-NTA-coupled agarose beads (Qiagen) (lane 2), Sepharose 4B beads alone (lane 3), or by monoclonal antibodies, BU63 (lane 4), and FUN-1 (lane 5), attached via protein A to Sepharose 4B beads. The visible bands present in lanes 4 and 5 appear to be the heavy and light chains of antibody dissociating from the beads.

(C) Elution of sB7-2 from a Sephadex S-200 gel-filtration column. The elution positions of size calibration markers are indicated.

### Analysis of sB7-2 Solution Properties by AUC

Deglycosylated sB7-1 forms a homodimer when crystallized alone (Ikemizu et al., 2000), as does fully glycosylated sB7-1 in solution and in crystal lattices when complexed with CTLA-4 (Ikemizu et al., 2000; Stamper et al., 2001). An unglycosylated form of B7-2, consisting of the ligand binding domain, forms asymmetric, back-to-back lattice contacts when cocrystallized with CTLA-4 (Schwartz et al., 2001). We therefore examined, using AUC, whether fully glycosylated sB7-2 produced in CHO cells is able to self-associate in solution. In equilibrium experiments at 37°C, neither sB7-2 (Figure 2A) nor the ICOS ligand, LICOS (Figure 2B), formed dimers or other oligomeric species. This conclusion was supported by sedimentation velocity experiments (data not shown) and gel-filtration analyses (e.g., Figure 1C). These results indicate that, in contrast to B7-1, the extracellular domain of glycosylated B7-2 does not self-associate.

### Stoichiometry of CD28Fc Interactions with sB7-1 and sB7-2

Early binding experiments (Linsley et al., 1995) and subsequent structural studies of CTLA-4/B7 complexes

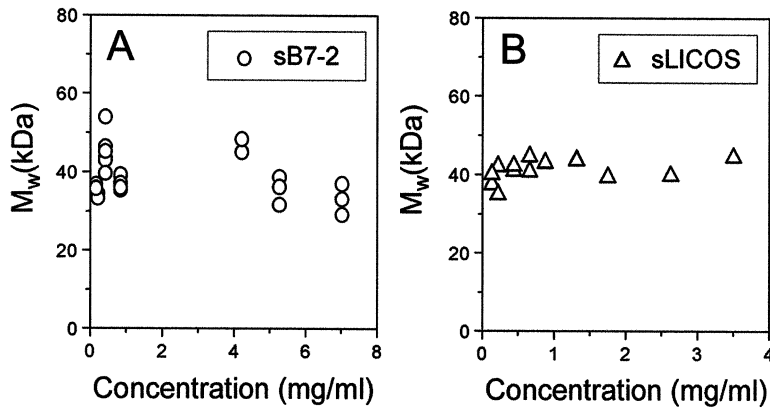


Figure 2. AUC Analysis of sB7-2 and sLICOS Molecular weights for sB7-2 (A) and sLICOS (B), determined from AUC equilibrium experiments, plotted against protein concentration.

(Stamper et al., 2001; Schwartz et al., 2001), have demonstrated unequivocally that the CTLA-4 homodimer is bivalent. While it is often assumed that the CD28 homodimer is also bivalent (Greene et al., 1996), this has never been directly demonstrated. We therefore analyzed the CD28 binding stoichiometry using surface plasmon resonance as implemented in the BIAcore. We compared the amount of sB7-1 that bound to given amounts of CD28Fc and CTLA-4Fc immobilized onto the BIAcore sensor surface (Figure 3A). A saturating amount of sB7-1 was injected over flow-cells in which CD28Fc, CTLA-4Fc, and a control protein were each immobilized. The difference in the level of the response in the CD28Fc or CTLA-4Fc flow-cells versus the control flow-cells represented the maximum level of sB7-1 binding. Since the level of sB7-1 binding depends on the level of active

immobilized CD28 or CTLA-4, this was determined by subsequently injecting saturating amounts of CD28- and CTLA-4-specific Fab' fragments. When normalized for the level of Fab' binding (sB7-1 binding/Fab' binding), it was evident that CTLA-4 bound twice the amount of sB7-1 than was bound by the equivalent level of CD28. Importantly, the CTLA-4 Fab' bound CTLA-4Fc that had been captured onto the BIAcore surface by the same Fab', indicating the presence of two epitopes on the CTLA-4Fc, as expected; similarly, the CD28 Fab' was shown to have two epitopes on CD28Fc (data not shown). Furthermore, the same 2-fold higher level of sB7-1 binding to CTLA-4 versus CD28 was observed when the normalization was performed with eight different CD28 antibodies and three different CTLA-4 antibodies (data not shown). These controls indicate that the

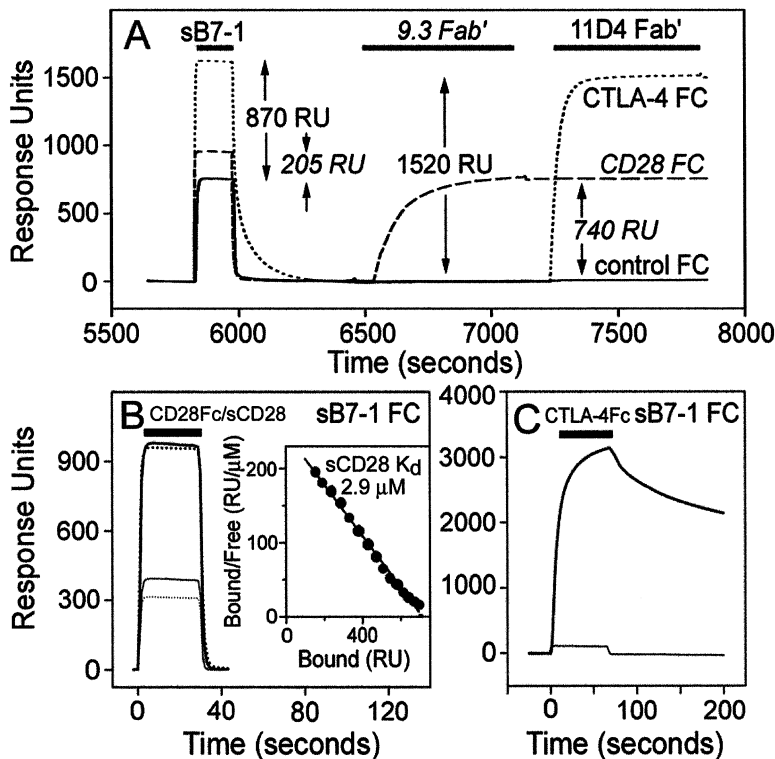


Figure 3. Stoichiometry of CD28 versus CTLA-4 Interactions

(A) A saturating amount of sB7-1 (42  $\mu$ M, solid bar) was injected through flow-cells in which CD28Fc (dashed line), CTLA-4Fc (dotted line), or CD22Fc (solid line) had been immobilized indirectly at 1529, 1703, and 1510 RUs, respectively. Following complete dissociation of sB7-1, 9.3 Fab' (anti-CD28) and 11D4 Fab' (anti-CTLA-4) were injected (solid bars) through all three flow-cells at saturating concentrations (50  $\mu$ g/ml). The amount of binding of sB7-1 was calculated by subtracting the background response in the CD22Fc flow-cell from the responses in the CD28Fc and CTLA-4Fc flow-cells. In the representative example shown, the ratio of CTLA-4/11D4 Fab' binding (870 RU/1520 RU = 0.57) is double that for CD28/9.3 Fab' binding (205 RU/740 RU = 0.28).  
(B) CD28Fc (4.3  $\mu$ M, solid lines) and sCD28 (20.1  $\mu$ M, dotted lines) were injected (solid bar) over a flow-cell containing directly immobilized sB7-1 (heavy lines) or control CD22Fc (light lines). Inset: For equilibrium binding analysis of the affinity of sCD28 for sB7-1, sCD28 was injected at a range of concentrations (44  $\mu$ M and 4/3-fold dilutions thereof) for 30 s at 10  $\mu$ l/min.  
(C) CTLA-4Fc (3  $\mu$ M) was injected (solid bar) over the flow-cells containing directly immobilized sB7-1 (heavy line) or control CD22Fc (light line).

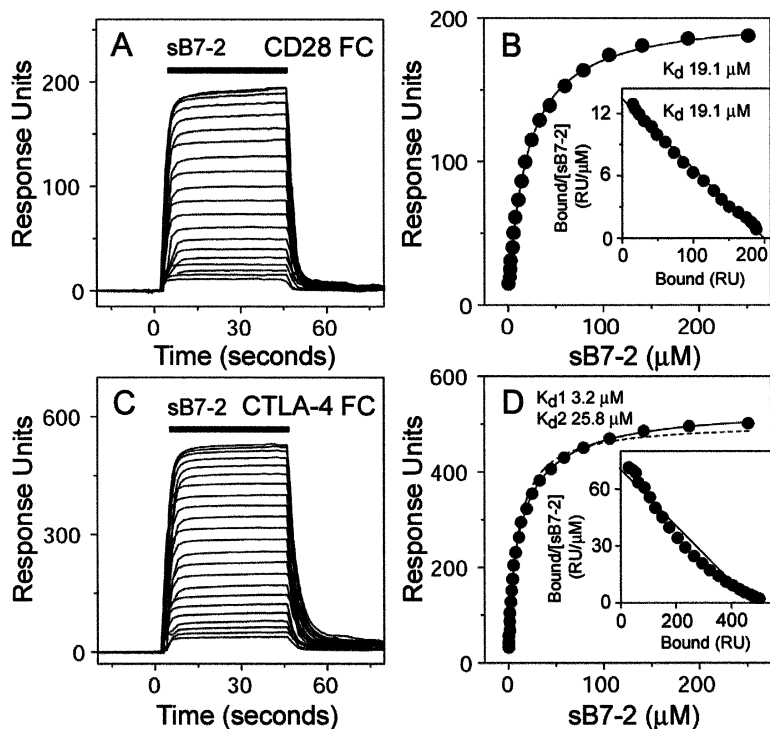


Figure 4. Equilibrium Binding Analyses

(A) sB7-2, at a range of concentrations (251 μM and 4/3-fold dilutions thereof) was injected at 10 μl/min sequentially (solid bar) through a flow-cell containing 2200 RU of indirectly immobilized CD28Fc at 37°C. Background responses observed in a control flow-cell containing immobilized CD22Fc were subtracted from the total responses to give binding (solid lines).

(B) Nonlinear curve fitting of the untransformed data using a 1:1 Langmuir binding isotherm yielded a  $K_d$  of 19.1 μM and a binding maximum of 203 RU. A linear Scatchard plot of the CD28/B7-2 binding data (inset) yielded the same  $K_d$  and binding maximum.

(C) sB7-2, at a range of concentrations (251 μM and 4/3-fold dilutions thereof) was injected as in (A) through a flow-cell containing 800 RU of indirectly immobilized CTLA-4Fc at 37°C. Background responses have been subtracted.

(D) Nonlinear curve fitting of the untransformed binding data using a 1:1 Langmuir binding isotherm (dashed line) gives a worse fit than a fixed, two-site binding model (solid line). The two-site model yielded high- and low-affinity  $K_d$  values of 3.2 and 25.8 μM, respectively. A Scatchard plot of the data (inset) was clearly nonlinear.

observed stoichiometry is not an artifact of an unusual antibody epitope. Significantly, there was also a 2-fold higher level of sB7-2 binding to CTLA-4Fc versus CD28Fc (data not shown), indicating that this difference in stoichiometry is identical for both sB7-1 and sB7-2.

These results, taken together with the known (2:1) stoichiometry of B7 binding to the CTLA-4 homodimer, indicate that only one B7 molecule binds a CD28 homodimer. If correct, this conclusion predicts that a soluble CD28 homodimer, because it is monovalent, would bind with the same properties to immobilized B7 as soluble B7 binds to immobilized CD28. To test this prediction, CD28Fc and CTLA-4Fc were injected over immobilized sB7-1 (Figures 3B and 3C). CD28Fc binding to immobilized sB7-1 displayed the same rapid kinetics observed when this interaction was studied in the reverse orientation (van der Merwe et al., 1997), reaching equilibrium within 10 s, and dissociating rapidly at the end of the injection (Figure 3B). In contrast, CTLA-4Fc bound immobilized sB7-1 with a much higher avidity than observed in the reverse orientation (van der Merwe et al., 1997), dissociating with a half-life ( $t_{1/2}$ ) > 200 s (Figure 3C) instead of ~2 s (van der Merwe et al., 1997).

In order to exclude an effect of the Fc region on the binding properties of the CD28, we also analyzed the binding of CD28 homodimer (sCD28) from which the Fc had been removed. sCD28 and CD28Fc bound with identical fast kinetics (Figure 3B). The affinity of sCD28 binding was measured by determining the binding at equilibrium of sCD28, at a range of concentrations, to immobilized sB7-1. A Scatchard plot of these data is linear (Figure 3B, inset), consistent with 1:1 binding, and gave a  $K_d$  value of  $4.2 \pm 0.9 \mu\text{M}$  (mean  $\pm$  SD,  $n = 5$ ), in excellent agreement with the  $K_d$  (4 μM) measured for sB7-1 binding to immobilized CD28Fc (van der Merwe

et al., 1997). In conclusion, the binding properties of sB7-1 binding to CD28 homodimer are independent of the binding orientation, consistent with a 1:1 binding stoichiometry. In contrast, sB7-1 binds with a higher avidity to CTLA-4 when sB7-1 is immobilized, consistent with a 1:2 CTLA-4Fc:sB7-1 stoichiometry. ICOSFc:sLICOS binding exhibited the same orientation dependence as CTLA-4Fc:sB7-1 interactions (data not shown), suggesting that this interaction also has a 1:2 stoichiometry.

#### Affinity Measurements

The affinity and kinetic properties of sB7-2:ligand interactions were also characterized using the BIAcore, with all experiments performed at 37°C except where indicated. The affinities were determined by equilibrium binding as this avoids pitfalls, such as mass-transport limitations and rebinding, which commonly affect kinetic measurements. To this end, sB7-2 at a wide range of concentrations was injected sequentially over immobilized CD28Fc or CTLA-4Fc (Figures 4A and 4C show overlays of the binding observed with the full range of sB7-2 concentrations). Binding reached equilibrium very quickly (>95% binding within 1–3 s) following the onset of the injection, and, when the injection ended, sB7-2 dissociated very rapidly, with near complete dissociation within 15 s (Figures 4A and 4C). A plot of the binding at equilibrium versus concentration indicated that the binding of sB7-2 to both CD28Fc and CTLA-4Fc was saturable (Figures 4B and 4D). For the sB7-2:CD28Fc binding data, an excellent fit of the 1:1 (Langmuir) binding isotherm (Figure 4B) was obtained by nonlinear curve fitting, and a Scatchard plot of the same data was linear (Figure 4B, inset). Thus, the binding conformed to the Langmuir binding model, and this indicated that both sB7-2 and CD28 were homogenous with a single type

of binding site. Successive, independent measurements yielded  $K_d$  values of  $20 \pm 2 \mu\text{M}$  (mean  $\pm$  SD,  $n = 4$ ), which is about 5-fold lower than the affinity measured for sB7-1 binding to CD28.

In contrast to the results obtained for sB7-2:CD28 binding, the sB7-2:CTLA-4Fc binding data did not conform to the Langmuir binding model (Figure 4D). This is evident in the poor nonlinear fit of the model to the untransformed binding data (Figure 4D) and the deviation from linearity of the Scatchard plot of the same data (Figure 4D, inset). There are numerous possible mechanisms that could account for such a result, including heterogeneity of sB7-2 and/or CTLA-4, or self-association of sB7-2. The fact that an excellent fit to the Langmuir model was observed with the same sB7-2 preparation binding to immobilized CD28Fc argues strongly against heterogeneity of sB7-2. Furthermore, as shown above, we were unable to detect any sB7-2 self-association. Thus, the most plausible explanation for the observed binding is heterogeneity of CTLA-4. Trivial explanations for CTLA-4 heterogeneity such as aggregation of CTLA-4 Fc or heterogeneous immobilization are unlikely since neither gel-filtration of the CTLA-4Fc immediately prior to immobilization nor indirect immobilization by an anti-Fc antibody eliminated this heterogeneous binding.

One possible source of the heterogeneous binding is the presence of two binding sites on a single CTLA-4Fc homodimer, each with distinct properties. Consistent with this, a simple two-site binding model gave a much better fit to the data than the one-site model ( $\text{Chi}^2 = 1.8$  versus 167 for two-site versus the one-site fits, Figure 4D, solid versus dashed line), and, in multiple fits, each site was at approximately a 1:1 ratio (1:1.22 for the fit shown in Figure 4D). The high- and low-affinity sites had  $K_d$  values of  $2.6 \pm 0.5 \mu\text{M}$  (mean  $\pm$  SD,  $n = 3$ ) and  $22.4 \pm 3 \mu\text{M}$  (mean  $\pm$  SD,  $n = 3$ ), respectively. Further support for a difference in the affinity between the two binding sites on the CTLA-4 homodimer was provided by re-analysis of previously published sB7-1 binding data (van der Merwe et al., 1997). While sB7-1 binding to CD28Fc fitted well to the Langmuir model, binding to CTLA-4Fc fitted significantly better to the simple two-site ( $\text{Chi}^2 = 3.3$ ) than to the one-site ( $\text{Chi}^2 = 56$ ) binding models and gave affinities for the two sites also differing  $\sim 7$ -fold in magnitude:  $0.2 \mu\text{M}$  and  $1.4 \mu\text{M}$  (data not shown). While the binding heterogeneity makes the comparison between B7-2 and B7-1 difficult, it is evident that B7-2 binds with a 10- to 20-fold lower affinity than B7-1 to CTLA-4.

These results indicate that sB7-2 and sB7-1 binding to CD28 is homogeneous whereas binding to CTLA-4 is heterogeneous. Affinity measurements of LICOS binding to immobilized ICOSFc, which appears to be bivalent, exhibited the same type of heterogeneity as B7 binding to immobilized CTLA-4Fc (data not shown).

#### Kinetic Measurements

Measurements of binding kinetics are more prone to error than equilibrium measurement, largely because of the problems of mass-transport limitations and rebinding of dissociated analyte, which can lead to the underestimation of binding rate constants. These artifacts can

be excluded if it is shown that decreasing the level of immobilized ligand does not result in an increase in the apparent rate constants.

#### CTLA-4Fc:sB7-2 Binding

Dissociation rate constants ( $k_{\text{off}}$ ) were determined following the injection of sB7-2 at a range of concentrations (Figure 5B). Good fits were obtained with a single exponential decay model, consistent with a single  $k_{\text{off}}$  value ( $\sim 5.1 \pm 0.8 \text{ s}^{-1}$  [mean  $\pm$  SD,  $n = 7$ ]). Importantly, this  $k_{\text{off}}$  was the same irrespective of the concentration at which the sB7-2 was injected (Figure 5B). These findings indicate that the CTLA-4 binding sites are homogenous with respect to their  $k_{\text{off}}$ . In separate experiments, we showed that the apparent  $k_{\text{off}}$  did not vary substantially when the level of immobilized CTLA-4 was varied around the values used for these measurements, ruling out mass-transport or rebinding artifacts (data not shown). Association-rate constants ( $k_{\text{on}}$ ) were determined by nonlinear curve fitting of the simple 1:1 Langmuir association model to injection-phase data using  $k_{\text{off}}$  values obtained from analysis of the corresponding dissociation phase (Figure 5A). Although reasonable fits were obtained, the small number of data points available for each fit before equilibrium is attained make it impossible to assess from individual fits whether the  $k_{\text{on}}$  values are heterogeneous. However, the finding that, unlike the  $k_{\text{off}}$  determinations, the measured apparent  $k_{\text{on}}$  values varied substantially with the concentration at which the sB7-2 was injected (Figure 5 legend), is evidence that the  $k_{\text{on}}$  is indeed heterogeneous. At the lowest sB7-2 concentration ( $6.5 \mu\text{M}$ ), the apparent  $k_{\text{on}}$  was 4-fold faster than at the highest sB7-2 concentration ( $105 \mu\text{M}$ ; Figure 5 legend). Since at low sB7-2 concentrations binding will primarily be to high-affinity sites whereas at higher concentrations binding will be to both high- and low-affinity sites, this indicates that the low- and high-affinity binding sites identified by equilibrium affinity measurements have similar  $k_{\text{off}}$  values but differ in their  $k_{\text{on}}$  values.

#### CD28Fc:sB7-2 Binding

sB7-2 dissociated extremely rapidly from immobilized CD28Fc such that the  $k_{\text{off}}$  was at the very limit of detection for the BIAcore. Several independent determinations gave a mean apparent  $k_{\text{off}}$  value of  $31 \pm 2$  (mean  $\pm$  SD,  $n = 4$ ; e.g., Figure 5C), a value that is indistinguishable from the theoretical wash rate at that flow rate ( $28 \text{ s}^{-1}$ ; Davis et al., 1998). Consequently, these rates must be considered to be the lower limit of the true  $k_{\text{off}}$  (i.e.,  $k_{\text{off}} \geq 28 \text{ s}^{-1}$ ). Binding was far too fast for the  $k_{\text{on}}$  to be measured directly. However, taking the  $k_{\text{off}}$  to be  $\geq 28 \text{ s}^{-1}$  and the  $K_d$  (determined by equilibrium binding analysis) to be  $20 \mu\text{M}$ , the  $k_{\text{on}}$  can be calculated to be  $\geq 1.4 \times 10^6 \text{ M}^{-1}\text{s}^{-1}$  at  $37^\circ\text{C}$ .

#### Discussion

The key findings of this study are summarized, along with the results of our previous analyses (van der Merwe et al., 1997; Ikemizu et al., 2000), in Figure 6. In discussing these results, we assume that the magnitude of the affinity differences we observe in solution apply equally to the equivalent interactions at the cell surface, as can be argued on theoretical grounds (Bell, 1978).

Our results indicate that B7-2 and B7-1 differ in three

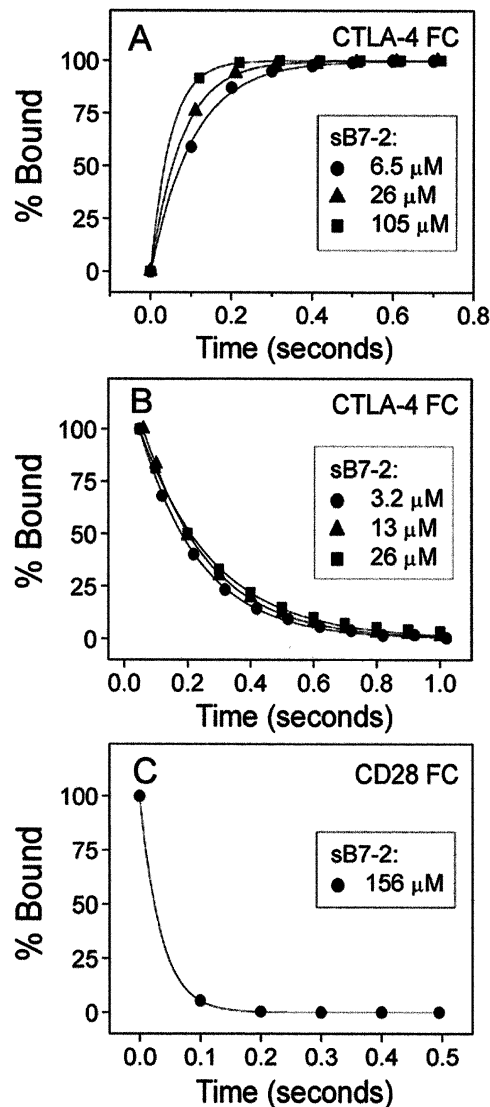


Figure 5. Kinetic Analysis of sB7-2 Binding to CTLA-4Fc and CD28Fc

(A) Nonlinear curve fitting of association data for sB7-2 injected at 6.5  $\mu\text{M}$ , 26  $\mu\text{M}$ , and 105  $\mu\text{M}$  over 1000 RU of directly immobilized CTLA-4Fc at 37°C. The data were fitted with standard 1:1 association models, giving  $k_{\text{on}}$  values of  $1.6 \times 10^5$ ,  $3.2 \times 10^5$ , and  $6.5 \times 10^5 \text{ M}^{-1}\text{s}^{-1}$  when sB7-2 was injected at 105, 26, and 6.5  $\mu\text{M}$ , respectively. (B) sB7-2, at concentrations of 3  $\mu\text{M}$ , 13  $\mu\text{M}$ , and 26  $\mu\text{M}$ , was injected at 100  $\mu\text{l}/\text{min}$  at 37°C over 1000 RU of directly immobilized CTLA-4Fc and allowed to dissociate at the end of each injection. Data were recorded at the maximal collection rate (10 Hz) until the response had returned to baseline. Responses in a control flow-cell were subtracted and the remaining binding plotted as a percentage of initial binding. The data are fitted with single exponential decay curves, giving  $k_{\text{off}}$  values of  $5.1 \pm 0.8 \text{ s}^{-1}$  (mean  $\pm$  SD,  $n = 7$ ). (C) Dissociation of sB7-2 from CD28Fc at 37°C. sB7-2 (156  $\mu\text{M}$ ) was injected over 1226 RU of immobilized CD28Fc at 100  $\mu\text{l}/\text{min}$ . The data are fitted with a single exponential decay curve yielding a  $k_{\text{off}}$  value of  $29.3 \text{ s}^{-1}$ .

key respects, each of which will markedly affect the signaling properties of CD28 and CTLA-4. First, B7-2 binds 13-fold more weakly to CTLA-4 than B7-1. Second, CTLA-4 interactions with B7-2, in contrast to those

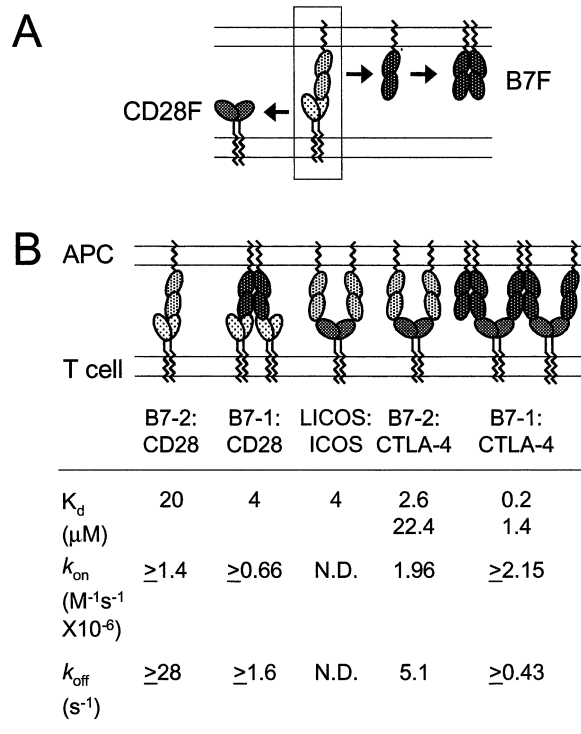


Figure 6. Summary of Organization and Binding Properties of Signaling Complexes Formed by CD28, CTLA-4, B7-1, B7-2, ICOS, and LICOS

(A) Proposed structural changes to B7 family (B7F) and CD28 family (CD28F) proteins in the course of their evolution. Gene duplication and sequence divergence yielded monomeric and homodimeric, low- and high-affinity forms of the B7 family. Similarly, gene duplication and structural rearrangements (see Figure 7) generated low-affinity monovalent and high-affinity bivalent members of the CD28 family. The proposed precursors (boxed) are based on the properties of the avian homologs of these proteins (i.e., chicken CD28 and chCD80L; D.W.B. and J. Young, unpublished data).

(B) Quaternary structures and binding properties of the signaling complexes formed by human CD28, CTLA-4, B7-1, B7-2, ICOS, and LICOS. The averaged affinities and measured or calculated kinetic constants for each interaction are also shown. The high- and low-affinity values shown for CTLA-4 interactions are for the two sites revealed by equilibrium binding analysis; only kinetic data relevant to the high-affinity binding site are presented. Data for B7-1 and LICOS interactions are from van der Merwe et al. (1997) and Brodie et al. (2000). N.D., not determined.

with B7-1, are unlikely to be avidity-enhanced by the formation of bivalent B7-2 homodimers capable of bridging CTLA-4 homodimers. Third, relative to its CTLA-4 binding affinity, B7-2 binds CD28 2- to 3-fold more effectively than B7-1 (i.e., the CD28/CTLA-4  $K_d$  ratios are  $\sim 8$  and 20 for B7-2 and B7-1, respectively). In other words, relative to B7-1, the binding of B7-2 is *biased* against CTLA-4. The consequence of this is that, all other things being equal, when B7-2 is expressed on an APC, the ratio of engaged CD28 to engaged CTLA-4 at the T cell:APC interface will be higher than when B7-1 is expressed. Activating signals elicited by B7-2:CD28 interactions are therefore less likely to be attenuated by coincident CTLA-4 ligation than those elicited by B7-1, enhancing the costimulatory effects of B7-2 when CD28 and CTLA-4 are coexpressed. Conversely, inhibitory sig-

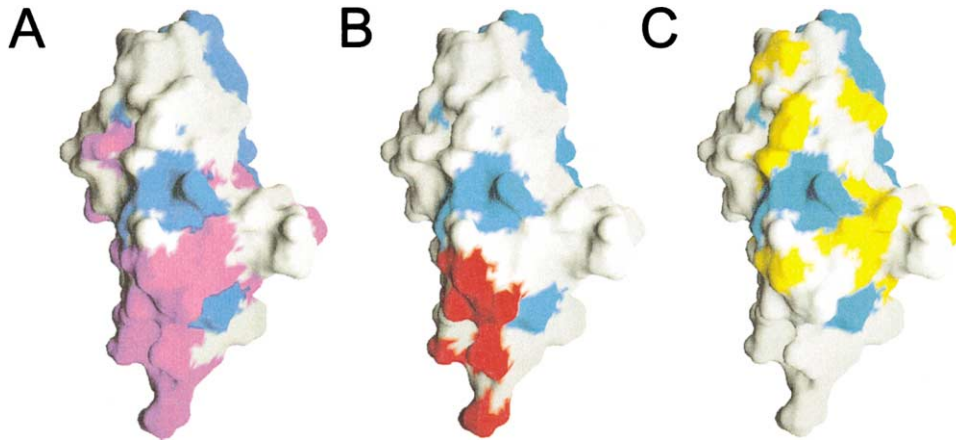


Figure 7. Surface Residue Conservation in CD28 and CTLA-4

In (A) through (C), a single view of the crystal structure of the CTLA-4 monomer is shown (Stamper et al., 2001). The line of view is parallel with the  $\beta$  sheets, with the ligand binding surface facing to the right and the COOH terminus at the base. Residues completely conserved in all CTLA-4 and CD28 homologs are colored blue. In (A), residues conserved in all CTLA-4 homologs and substituted in one or more of the CD28 homologs are colored pink. In (B), residues mediating CTLA-4 homodimerization (a subset of those colored pink in (A)) are colored red. In (C), CD28-equivalent residues conserved in all CD28 homologs and substituted in one or more of the CTLA-4 homologs are colored yellow. The absence in CD28 of any conservation of the residues mediating the formation of CTLA-4 homodimers suggests that CD28 may self-associate into homodimers that are structurally distinct from those of CTLA-4.

naling by B7-1 will be enhanced under the same circumstances. Taken together, these results indicate that B7-1 interactions with CTLA-4 will be markedly favored over interactions with CD28 and that B7-2 will exhibit much less bias. We conclude, therefore, that the delayed expression of B7-1 is timed to specifically enhance inhibitory signaling by CTLA-4.

The concept that, by preferentially engaging CTLA-4, B7-1 is predominantly but not exclusively inhibitory, whereas B7-2 is costimulatory due to more effective interactions with CD28, is compatible with a number of studies in which the properties of B7-1 and B7-2 have been compared. We cite just a few *in vivo* experiments as examples: (1) treatment of NOD mice with blocking anti-B7-2 mAb protects from diabetes whereas blocking anti-B7-1 accelerates the disease process in female mice and induces diabetes in normally resistant males (Lenschow et al., 1995); (2) antigen-dependent expansion of adoptively transferred, transgenic CD4<sup>+</sup> T cells is enhanced by anti-B7-1 mAb and partially inhibited by anti-B7-2 (Kearney et al., 1995); (3) in a murine model of allo-transplantation, B7-1 and CTLA-4 are necessary for tolerance induction whereas B7-2 is required for activation of the allo-reactive T cells (Judge et al., 1999); and (4) B7-2-deficient mice have milder kidney damage than wild-type mice, in contrast to B7-1-deficient mice which have more severe damage in a murine systemic erythematosis model (Liang et al., 1999). We acknowledge, however, that in some systems B7-2 blockade enhances immune responses and that anti-B7-1 antibodies are inhibitory. For example, experimental allergic encephalomyelitis, autoimmune uveoretinitis, and crescentic glomerulonephritis are all more severe in anti-B7-2 than anti-B7-1 mAb-treated mice (Kuchroo et al., 1995; Fukai et al., 1999; Li et al., 2000). Restricting or enhancing the development of protective TH2 responses, by interfering with the preferential interactions of CD28 and CTLA-4 with B7-2 and B7-1, may pro-

foundly alter the course of disease in these TH1-dependent models, however. These issues will be discussed at length elsewhere.

Whereas the present study indicates that the structures and ligand binding properties of B7-1 and B7-2 are very different, others have emphasized their similarities. Linsley et al. (1994) concluded on the basis of multivalent assays that B7-1 and B7-2 bind with similar avidities to CD28 versus CTLA-4. We note, however, that assays of this type will inevitably tend to conceal real affinity differences. Similarly, Schwartz et al. (2001) proposed that B7-2 forms B7-1-like homodimers on the basis of lattice contacts observed in crystals of bacterially expressed B7-2 domain 1:CTLA-4 complexes. While superficially similar to sB7-1 homodimers, the B7-2 homodimers and CTLA-4:B7-2 interfaces were structurally asymmetric, contrary to the expectation that organized, self-assembled structures form via identical subunit interactions (Klug, 1969). Unconstrained, asymmetric structures, such as those proposed to form at the cell surface for B7-2, will fail to efficiently self-assemble because lower-energy conformations will always be favored over higher-energy states. We predict that native sB7-2 does not dimerize because it is glycosylated at the base of the dimer interface proposed by Schwartz et al. (2001) (i.e., at Asn-8). This site will be unglycosylated in bacterially expressed protein, implying that the B7-2 homodimers are artifacts of crystallization.

The observation that CD28 homodimers are monovalent whereas CTLA-4 is bivalent was unexpected given the generally accepted view that these molecules are each bivalent (see, e.g., Sharpe and Freeman, 2002; Carreno and Collins, 2002). Greene et al. (1996) were the first to propose two-site binding models for both CTLA-4 and CD28. Crucially, however, Greene et al. were uncertain whether their CD28 preparation was dimeric or tetrameric. This is important as the presence of even small amounts of bivalent tetramers would account

for the CD28 binding heterogeneity observed in their experiments.

The effect of bivalency on the avidity of interacting cell surface molecules is difficult to measure or calculate. A reasonable guide, based on the solution off-rates for the binding of monovalent versus bivalent forms of CTLA-4 to immobilized sB7-1, is that bivalent binding is approximately two orders of magnitude more stable than monovalent binding (the  $t_{1/2}$  values for the dissociation of monomeric CTLA-4 and CTLA-4Fc from immobilized sB7-1, are  $\sim 2$  s [data not shown] and  $>200$  s [Figure 3C], respectively). Overall, the monovalent affinities of interactions within this system vary up to 100-fold in magnitude (i.e., from low-affinity B7-2:CD28 interactions of  $K_d = 20 \mu\text{M}$  to high-affinity B7-1:CTLA-4 interactions of  $K_d = 0.2 \mu\text{M}$ ). The effects of bivalent binding by CTLA-4 will extend this range of stabilities, perhaps by two orders of magnitude. Bivalent B7-1 interactions will further enhance these effects. The sequential expression of B7-2 and B7-1, allied with these quaternary structural and affinity differences, are therefore likely to effect  $>10,000$ -fold differences in the half-lives of these closely related signaling complexes.

Why might such profound changes in the stability of the signaling complexes be necessary? The CD28:B7-2 interaction ( $K_d = 20 \mu\text{M}$ ) has similar properties to TCR- and adhesion molecule (CD2)-ligand interactions; i.e., binding is monovalent and has fast kinetics and similarly high  $K_d$  values ( $15\text{--}20 \mu\text{M}$ ; Willcox et al., 1999; van der Merwe et al., 1994). Interactions with these properties are ideally suited to highly dynamic cell-cell contacts that will facilitate the "scanning" of cellular targets for antigenic and adhesive ligands early in immune responses (van der Merwe et al., 1995; Davis et al., 1998). It is possible that the discrimination between various types of antigen-presenting cells, e.g., by scanning for the expression of B7 molecules, is another early event influencing the course of T cell responses, that is likely to be enhanced by such interactions. Naive T cells, however, express relatively little CD28, and it has been suggested that B7:CD28 interactions are TCR- and immunological synapse dependent (Bromley et al., 2001). In this context, the very low affinity of CD28:B7-2 interactions might instead ensure that costimulatory CD28 signaling does not preempt or overwhelm TCR responses given that the two signaling pathways apparently intersect (Hegner et al., 2000). In contrast to CD28:B7-2 interactions, the combination of submicromolar affinity and oligomeric, avidity-driven binding is thus far unique to B7-1:CTLA-4 interactions. The biochemistry of inhibitory signaling may require relatively prolonged receptor ligation to overturn ongoing activation signals. In this case, the formation of relatively few, very stable complexes might permit efficient inhibitory signaling without compromising the need for reversible cell-cell contact. We note that, compared to CD28:B7-2 and CTLA-4:B7-1 complexes, CD28:B7-1 and CTLA-4:B7-2 complexes will be intermediate in strength because CD28 is monovalent and B7-2 does not self-associate (Figure 6). The formation of such complexes might be important in allowing the intensity of costimulatory or inhibitory signaling to be varied with the stage of T cell or APC differentiation.

Finally, the structural basis of the stoichiometric differ-

ences between CD28 and CTLA-4 is unresolved. One possibility is suggested by our analysis of B7:CTLA-4 interactions, which shows that B7 proteins bind with two on-rates and a single off-rate. The simplest explanation for this is that the two binding sites are equivalent but that binding of the first B7 molecule to CTLA-4 reduces the on-rate for binding of the second. The structures of B7:CTLA-4 complexes (Schwartz et al., 2001; Stamper et al., 2001) reveal that the B7 molecules bind in the same plane and parallel to one another, allowing steric interference with association of the second molecule. Since the MYPPPY sequence at the heart of the binding face is conserved in both CD28 and CTLA-4, it is very likely that the B7 proteins bind CD28 monomers in much the same way. However, the two monomers might be organized differently in CD28, exaggerating the interference seen in CTLA-4 interactions, to the extent that binding of a second B7 molecule is completely prevented. Consistent with this possibility, we note that the most conserved surface residues outside the binding face of CD28 map not to the base of the A- and G- $\beta$  strands, which, along with a disulphide bond, mediate CTLA-4 homodimerization (Figures 7A and 7B), but to the top of these strands (Figure 7C), suggesting a distinct arrangement of the CD28 monomers.

Predicting when such a rearrangement might have occurred in the course of the evolution of these proteins is more difficult. It is clear that CD28, CTLA-4, and ICOS evolved from a common precursor, as did the B7-proteins and LICOS. The bivalency of CTLA-4 and ICOS (D.W.B. and A.V.C., unpublished data) suggests that the common precursor was bivalent. However, preliminary studies (D.W.B. and J.R. Young, unpublished data) showing that chicken CD28 binds monovalently to the putative LICOS homolog, chCD80L (O'Regan et al., 1999), imply that the most ancient form was monovalent (Figure 6A). Regardless of when it might have occurred, the switch between monovalent and bivalent binding is likely to have had the largest single effect on the relative strength of these interactions. A structural change of this type could well have initiated the functional diversification of this signaling system.

## Experimental Procedures

### Expression of sB7-2

DNA encoding the extracellular region of B7-2 (sB7-2) was amplified by polymerase chain reaction (PCR) from cDNA prepared from MT-2 cells. The 5' primer was complementary to the B7-2 leader sequence (MDPQCTMG), and we added a BamHI site and inserted, immediately upstream of the initiation codon, the 25 bases that precede the rat CD4 initiation codon. The 3' primer was complementary to the membrane proximal, LEDPQPPP-encoding sequence, and we added codons encoding a tag consisting of an arginine residue followed by six histidines, a stop codon, and a second XbaI site. The PCR fragment was sequenced and subcloned into the glutamine synthetase-based gene expression vector, pEE14, as described for sB7-1 (van der Merwe et al., 1997).

CHO-K1 cells were transfected using the calcium phosphate method, and clones expressing the most sB7-2 were selected by Western blotting using the ECL detection system (Amersham-Pharmacia Biotech [APB], Freiburg, Germany). The best clone was grown to confluence in bulk culture before switching to fresh medium in the presence of 2 mM sodium butyrate. The supernatant was harvested after approximately 4 weeks and the sB7-2 extracted by affinity chromatography using Ni-NTA agarose (Qiagen Ltd, Crawley,

UK). The sB7-2 was eluted from the Ni-NTA agarose with 250 mM imidazole (Sigma-Aldrich, St. Louis, MO) and further purified by passing the protein over a HiTrap Blue column (APB) to remove contaminating albumin, followed by size exclusion chromatography (Superdex 200 HR 10/30 column, APB). The extinction coefficient was determined by amino acid analysis to be 0.904 ml/mg. Prior to BIAcore analysis, the sB7-2 was re-passed over the Superdex 200 gel filtration column to remove aggregated protein.

#### General SPR Experiments

Binding experiments were carried out using surface plasmon resonance as implemented in the BIAcore 2000 and 3000 (BIAcore AB, St. Albans, UK). Affinity and kinetic analyses were performed at 25°C and 37°C in HBS-EP buffer (25 mM HEPES [pH 7.4], 150 mM NaCl, 3.4 mM EDTA, and 0.005% surfactant P20) (BIAcore AB). For experiments to determine the binding affinity of sB7-2 for its ligands, CTLA-4Fc and CD28Fc (kind gifts of P.S. Linsley), or control Fc proteins, were indirectly immobilized to the sensor surface via the anti-human IgG, monoclonal antibody (r10z8e9), as previously described (van der Merwe et al., 1997). The antibody (25 µg/ml in 10 mM sodium acetate [pH 4.0]) was directly immobilized to the dextran matrix of research grade CM5 sensor chips (BIAcore AB) by amine coupling using the manufacturer's kit (BIAcore AB) and an activation time of 5 min, resulting in immobilization levels of ~750–2200 response units (RU). Following coupling, CD28Fc, CTLA-4Fc, or control protein was passed through individual flow-cells until immobilized via the Ig Fc portion of each protein at the required level. For kinetic analyses, CD28Fc, CTLA-4Fc, and control proteins (20 µg/ml in 10 mM sodium acetate [pH 4.8]) were directly immobilized to the sensor chip surface by amine coupling using the manufacturer's kit and an activation time of 5 min, resulting in immobilization levels of ~500–1200 RUs. sB7-1 and sB7-2 (~20 µg/ml in 10 mM sodium acetate [pH 5]) were also directly immobilized by amine coupling to levels of ~3000 RU. Fab' fragments were prepared using an ImmunoPure Fab Preparation Kit (Pierce, Rockford, IL) and were immobilized by amine coupling (30–50 µg/ml in 10 mM sodium acetate [pH 4–4.5]) to levels of 500–900 RUs.

Equilibrium binding analysis was undertaken as described (van der Merwe et al., 1997). In brief, serial dilutions of sB7-2 were injected simultaneously over flow-cells containing indirectly immobilized CTLA-4Fc, CD28Fc, or control protein (CD22-Fc) at 25°C and 37°C. Injections were of 1 min duration, at a buffer flow rate of 10 µl/min, which proved sufficient to allow binding to reach equilibrium. For the kinetic analyses, dissociation rates were measured as described (van der Merwe et al., 1997). The binding data were examined using BIAevaluation software (BIAcore) and affinity and kinetic parameters derived using the curve fitting tools of Origin v.5.0 (MicroCal Software Inc., Northampton, MA).

The following equations were used for nonlinear curve fitting of the equilibrium affinity data:

$$B = B_{\max} \left( \frac{F}{F + K_d} \right) \text{ Langmuir one-site model} \quad (1)$$

$$B = B_{\max} \left( \frac{F}{F + K_{d1}} \right) + B_{\max2} \left( \frac{F}{F + K_{d2}} \right) \text{ Two-site model} \quad (2)$$

Where B is bound analyte (in RUs),  $B_{\max}$  is maximum binding of analyte, F is free analyte concentration (in µM), and  $K_d$  is the equilibrium dissociation constant (in µM). In the two-site model, each site has its own  $B_{\max}$  and  $K_d$  value.

The following equations were used for nonlinear curve fitting of the kinetic data.

For the association phase:

$$B_t = B_e^* (1 - e^{-(k_{on}F + k_{off})t}) \quad (3)$$

For the dissociation phase:

$$B_t = B_0 (1 - e^{-k_{off}t}) \quad (4)$$

Where  $B_0$ ,  $B_t$ , and  $B_e$  are bound analyte at time zero, time t, and at equilibrium.

#### Analytical Ultracentrifugation Methods

Sedimentation equilibrium experiments were performed in a Beckman Optima XL-I analytical ultracentrifuge essentially as previously described (Ikemizu et al., 2000). LICOS and sB7-2 were investigated at a range of concentrations, and data were collected at a number of wavelengths, ensuring linearity of absorbance:concentration. The sample distributions measured at equilibrium were fitted with a model for a single, ideal species. Self-association thus manifests as rising whole-cell molecular weights (Ikemizu et al., 2000). The data were fitted directly to the equation

$$A(r) = A(r_r) \exp \left[ \frac{(1 - \bar{v}\rho)\omega^2}{2RT} (r^2 - r_r^2) \right] + E \quad (5)$$

(where  $A(r)$  is the absorbance at radius  $r$  [in cm],  $A(r_r)$  is the absorbance at reference radius  $r_r$ ,  $\bar{v}$  is the partial specific volume [in ml/g],  $\rho$  is the solvent density [in g/ml],  $\omega$  is the angular velocity of the centrifuge rotor [in rad/sec],  $R$  is the gas constant,  $T$  is the absolute temperature, and  $E$  is the baseline offset) using either the nonlinear, least squares curve-fitting package Profit or the program ULTRASPIN (D.B. Veprintsev, N.W. Foster, and A.R. Fersht, personal communication). The  $\bar{v}$  was determined experimentally by comparing the mass of a protein from MALDI-TOF mass spectrometry with its known sequence mass and was the same as that calculated previously for sB7-1 (Ikemizu et al., 2000).

#### Acknowledgments

The authors thank, P. Bjork, P. Sørensen, and K. Uvebrant for helpful comments on the manuscript, E. Evans for assistance with the preparation of Figure 7, and Alice Kearney for help with some of the BIAcore experiments. This work was funded by the United Kingdom Arthritis Research Campaign, the Medical Research Council, and The Wellcome Trust.

Received: November 14, 2001

Revised: July 12, 2002

#### References

- Bachmann, M.F., Kohler, G., Ecabert, B., Mak, T.W., and Kopf, M. (1999). Cutting edge: lymphoproliferative disease in the absence of CTLA-4 is not T cell autonomous. *J. Immunol.* 163, 1128–1131.
- Bell, G.I. (1978). Models for the specific adhesion of cells to cells. *Science* 200, 618–627.
- Boise, L.H., Minn, A.J., Noel, P.J., June, C.H., Accavitti, M.A., Lindsten, T., and Thompson, C.B. (1995). CD28 costimulation can promote T cell survival by enhancing the expression of Bcl-XL. *Immunity* 3, 87–98.
- Borriello, F., Sethna, M.P., Boyd, S.D., Schweitzer, A.N., Tivol, E.A., Jacoby, D., Strom, T.B., Simpson, E.M., Freeman, G.J., and Sharpe, A.H. (1997). B7-1 and B7-2 have overlapping, critical roles in immunoglobulin class switching and germinal center formation. *Immunity* 6, 303–313.
- Brodie, D., Collins, A.V., Iaboni, A., Fennelly, J.A., Sparks, L.M., Xu, X.N., van der Merwe, P.A., and Davis, S.J. (2000). LICOS, a primordial costimulatory ligand? *Curr. Biol.* 10, 333–336.
- Bromley, S.K., Iaboni, A., Davis, S.J., Whitty, A., Green, J.M., Shaw, A.S., Weiss, A., and Dustin, M.L. (2001). The immunological synapse and CD28–CD80 interactions. *Nat. Immunol.* 2, 1159–1166.
- Carreno, B.M., and Collins, M. (2002). The B7 family of ligands and its receptors: new pathways for costimulation and inhibition of immune responses. *Annu. Rev. Immunol.* 20, 29–53.
- Davis, S.J., Ikemizu, S., Wild, M.K., and van der Merwe, P.A. (1998). CD2 and the nature of protein interactions mediating cell-cell recognition. *Immunol. Rev.* 163, 217–236.
- Fukai, T., Okada, A.A., Sakai, J., Kezuka, T., Keino, H., Usui, M., Yagita, H., Okumura, K., and Mizuguchi, J. (1999). The role of costimulatory molecules B7-1 and B7-2 in mice with experimental autoimmune uveoretinitis. *Graefes Arch. Clin. Exp. Ophthalmol.* 237, 928–933.
- Greene, J.L., Leytze, G.M., Emswiler, J., Peach, R., Bajorath, J.,

- Cosand, W., and Linsley, P.S. (1996). Covalent dimerization of CD28/CTLA-4 and oligomerization of CD80/CD86 regulate T cell costimulatory interactions. *J. Biol. Chem.* *271*, 26762–26771.
- Hegner, S.P., Hofmann, T.G., Dienz, O., Droge, W., and Schmitz, M.L. (2000). Tyrosine-phosphorylated Vav1 as a point of integration for T-cell receptor- and CD28-mediated activation of JNK, p38, and interleukin-2 transcription. *J. Biol. Chem.* *275*, 18160–18171.
- Hutloff, A., Dittrich, A.M., Beier, K.C., Eljaschewitsch, B., Kraft, R., Anagnostopoulos, I., and Kroczeck, R.A. (1999). ICOS is an inducible T-cell co-stimulator structurally and functionally related to CD28. *Nature* *397*, 263–266.
- Ikemizu, S., Gilbert, R.J.C., Fennelly, J.A., Collins, A.V., Harlos, K., Jones, E.Y., Stuart, D.I., and Davis, S.J. (2000). Structure and dimerization of a soluble form of B7-1. *Immunity* *12*, 51–60.
- Jenkins, M.K. (1994). The ups and downs of T cell costimulation. *Immunity* *1*, 443–446.
- Judge, T.A., Wu, Z., Zheng, X.G., Sharpe, A.H., Sayegh, M.H., and Turka, L.A. (1999). The role of CD80, CD86, and CTLA4 in alloimmune responses and the induction of long-term allograft survival. *J. Immunol.* *162*, 1947–1951.
- Kearney, E.R., Walunas, T.L., Karr, R.W., Morton, P.A., Loh, D.Y., Bluestone, J.A., and Jenkins, M.K. (1995). Antigen-dependent clonal expansion of a trace population of antigen-specific CD4+ T cells in vivo is dependent on CD28 costimulation and inhibited by CTLA-4. *J. Immunol.* *155*, 1032–1036.
- Klug, A. (1969). Point groups and the design of aggregates. In Nobel Symposium 11: Symmetry and Function of Biological Systems at the Macromolecular Level. A. Engstroem and B. Strandberg, eds., pp. 425–436.
- Kuchroo, V.K., Das, M.P., Brown, J.A., Ranger, A.M., Zamvil, S.S., Sobel, R.A., Weiner, H.L., Nabavi, N., and Glimcher, L.H. (1995). B7-1 and B7-2 costimulatory molecules activate differentially the Th1/Th2 developmental pathways: application to autoimmune disease therapy. *Cell* *80*, 707–718.
- Lee, K.M., Chuang, E., Griffin, M., Khattry, R., Hong, D.K., Zhang, W., Straus, D., Samelson, L.E., Thompson, C.B., and Bluestone, J.A. (1998). Molecular basis of T cell inactivation by CTLA-4. *Science* *282*, 2263–2266.
- Lenschow, D.J., Ho, S.C., Sattar, H., Rhee, L., Gray, G., Nabavi, N., Herold, K.C., and Bluestone, J.A. (1995). Differential effects of anti-B7-1 and anti-B7-2 monoclonal antibody treatment on the development of diabetes in the nonobese diabetic mouse. *J. Exp. Med.* *181*, 1145–1155.
- Lenschow, D.J., Walunas, T.L., and Bluestone, J.A. (1996). CD28/B7 system of T cell costimulation. *Annu. Rev. Immunol.* *14*, 233–258.
- Li, S., Holdsworth, S.R., and Tipping, P.G. (2000). B7.1 and B7.2 costimulatory molecules regulate crescentic glomerulonephritis. *Eur. J. Immunol.* *30*, 1394–1401.
- Liang, B., Gee, R.J., Kashgarian, M.J., Sharpe, A.H., and Mamula, M.J. (1999). B7 costimulation in the development of lupus: autoimmunity arises either in the absence of B7.1/B7.2 or in the presence of anti-B7.1/B7.2 blocking antibodies. *J. Immunol.* *163*, 2322–2329.
- Lindstein, T., June, C.H., Ledbetter, J.A., Stella, G., and Thompson, C.B. (1989). Regulation of lymphokine messenger RNA stability by a surface-mediated T cell activation pathway. *Science* *244*, 339–343.
- Linsley, P.S., Greene, J.L., Brady, W., Bajorath, J., Ledbetter, J.A., and Peach, R. (1994). Human B7-1 (CD80) and B7-2 (CD86) bind with similar avidities but distinct kinetics to CD28 and CTLA-4 receptors. *Immunity* *1*, 793–801.
- Linsley, P.S., Nadler, S.G., Bajorath, J., Peach, R., Leung, H.T., Rogers, J., Bradshaw, J., Stebbins, M., Leytze, G., Brady, W., et al. (1995). Binding stoichiometry of cytotoxic T lymphocyte-associated molecule-4 (CTLA-4). A disulphide-linked homodimer binds two CD86 molecules. *J. Biol. Chem.* *270*, 15417–15424.
- Mandelbrot, D.A., McAdam, A.J., and Sharpe, A.H. (1999). B7-1 or B7-2 is required to produce the lymphoproliferative phenotype in mice lacking cytotoxic T lymphocyte-associated antigen 4 (CTLA-4). *J. Exp. Med.* *189*, 435–440.
- Marengere, L.E., Waterhouse, P., Duncan, G.S., Mittrucker, H.W., Feng, G.S., and Mak, T.W. (1996). Regulation of T cell receptor signaling by tyrosine phosphatase SYP association with CTLA-4. *Science* *272*, 1170–1173.
- Masteller, E.L., Chuang, E., Mullen, A.C., Reiner, S.L., and Thompson, C.B. (2000). Structural analysis of CTLA-4 function in vivo. *J. Immunol.* *164*, 5319–5327.
- Mueller, D.L. (2000). T cells: a proliferation of costimulatory molecules. *Curr. Biol.* *10*, R227–R230.
- O'Regan, M.N., Parsons, K.R., Tregaskes, C.A., and Young, J.R. (1999). A chicken homologue of the co-stimulating molecule CD80 which binds to mammalian CTLA-4. *Immunogenetics* *49*, 68–71.
- Read, S., Malmstrom, V., and Powrie, F. (2000). Cytotoxic T lymphocyte-associated antigen 4 plays an essential role in the function of CD25(+)CD4(+) regulatory cells that control intestinal inflammation. *J. Exp. Med.* *192*, 295–302.
- Salomon, B., and Bluestone, J.A. (2001). Complexities of CD28/B7: CTLA-4 costimulatory pathways in autoimmunity and transplantation. *Annu. Rev. Immunol.* *19*, 225–252.
- Schwartz, J.C., Zhang, X., Fedorov, A.A., Nathenson, S.G., and Almo, S.C. (2001). Structural basis for co-stimulation by the human CTLA-4/B7-2 complex. *Nature* *410*, 604–608.
- Shapiro, V.S., Truitt, K.E., Imboden, J.B., and Weiss, A. (1997). CD28 mediates transcriptional upregulation of the interleukin-2 (IL-2) promoter through a composite element containing the CD28RE and NF-IL-2B AP-1 sites. *Mol. Cell. Biol.* *17*, 4051–4058.
- Sharpe, A.H., and Freeman, G.J. (2002). The B7–CD28 superfamily. *Nat. Rev. Immunol.* *2*, 116–126.
- Stamper, C.C., Zhang, Y., Tobin, J.F., Erbe, D.V., Ikemizu, S., Davis, S.J., Stahl, M.L., Seehra, J., Somers, W.S., and Mosyak, L. (2001). Crystal structure of the B7-1/CTLA-4 complex that inhibits human immune responses. *Nature* *410*, 608–611.
- Takahashi, T., Tagami, T., Yamazaki, S., Uede, T., Shimizu, J., Sakaguchi, N., Mak, T.W., and Sakaguchi, S. (2000). Immunologic self-tolerance maintained by CD25(+)CD4(+) regulatory T cells constitutively expressing cytotoxic T lymphocyte-associated antigen 4. *J. Exp. Med.* *192*, 303–310.
- van der Merwe, P.A., Barclay, A.N., Mason, D.W., Davies, E.A., Morgan, B.P., Tone, M., Krishnam, A.K., Ianelli, C., and Davis, S.J. (1994). Human cell-adhesion molecule CD2 binds CD58 (LFA-3) with a very low affinity and an extremely fast dissociation rate but does not bind CD48 or CD59. *Biochemistry* *33*, 10149–10160.
- van der Merwe, P.A., McNamee, P.N., Davies, E.A., Barclay, A.N., and Davis, S.J. (1995). Topology of the CD2–CD48 cell-adhesion molecule complex: implications for antigen recognition by T cells. *Curr. Biol.* *5*, 74–84.
- van der Merwe, P.A., Bodian, D.L., Daenke, S., Linsley, P.S., and Davis, S.J. (1997). B7-1 (CD80) binds both CD28 and CTLA-4 with a low affinity and very fast kinetics. *J. Exp. Med.* *185*, 393–403.
- Viola, A., Schroeder, S., Sakakibara, Y., and Lanzavecchia, A. (1999). T lymphocyte costimulation mediated by reorganization of membrane microdomains. *Science* *283*, 680–682.
- Waterhouse, P., Penninger, J.M., Timms, E., Wakeham, A., Shahinian, A., Lee, K.P., Thompson, C.B., Griesser, H., and Mak, T.W. (1995). Lymphoproliferative disorders with early lethality in mice deficient in CtlA-4. *Science* *270*, 985–988.
- Willcox, B.E., Gao, G.F., Wyer, J.R., Ladbury, J.E., Bell, J.I., Jakobsen, B.K., and van der Merwe, P.A. (1999). TCR binding to peptide-MHC stabilizes a flexible recognition interface. *Immunity* *10*, 357–365.
- Wülfing, C., and Davis, M.M. (1999). A receptor/cytoskeletal movement triggered by costimulation during T cell activation. *Science* *282*, 2266–2269.